




# Self-Assembly of Chiral Menthol Molecules from a Liquid Film into Ring-Banded Spherulites

Tamás Kovács,<sup>†,‡</sup> Rózsa Szűcs,<sup>§</sup> Gábor Holló,<sup>||</sup> Zita Zuba,<sup>⊥</sup> János Molnár,<sup>⊥</sup> Hugo K. Christenson,<sup>†</sup> and István Lagzi<sup>\*,||,#</sup> 

<sup>†</sup>School of Physics and Astronomy, University of Leeds, LS2 9JT Leeds, United Kingdom

<sup>‡</sup>Laboratory for Chemical Kinetics, Eötvös Loránd University, Pázmány Péter sétány 1/A, H-1117 Budapest, Hungary

<sup>§</sup>MTA-BME Computer Driven Chemistry, Budapest University of Technology and Economics, Szent Gellért tér 4, H-1111 Budapest, Hungary

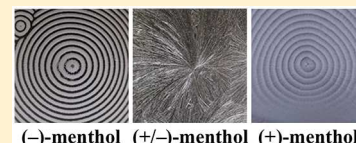
<sup>||</sup>MTA-BME Condensed Matter Research Group, Budapest University of Technology and Economics, Budafoki út 8, H-1111 Budapest, Hungary

<sup>⊥</sup>Department of Physical Chemistry and Materials Science, Budapest University of Technology and Economics, Műegyetem rkp. 3, H-1111 Budapest, Hungary

<sup>#</sup>Department of Physics, Budapest University of Technology and Economics, Budafoki út 8, H-1111 Budapest, Hungary

## Supporting Information

**ABSTRACT:** We investigate the growth of spherulites in the wake of a solidification front in a thin film of liquid menthol. We observed that the two enantiomeric forms of menthol ((-)-menthol and (+)-menthol) form ring-banded spherulites, in which needle-like crystals self-assemble into high- and low-density crystal regions. Interestingly, the racemic mixture produces nonbanded spherulites consisting of closely packed plate-like crystals. In the ring-banded spherulitic growth, we could clearly identify the curvature effect of the solidification front on the pattern formation on a millimeter spatial scale. We developed a numerical model based on the Cahn–Hilliard equation, which qualitatively describes the main features observed in experiments, namely, the formation of periodic ring-banded structures and the curvature effect of the propagating solidification front.



## ■ INTRODUCTION

Phase transitions (including crystallization and solidification) are general phenomena in nature and in the laboratory that have a significant effect on natural processes and on applications in industrial processes (e.g., zone melting, polymer formation).<sup>1</sup> At a given pressure, a liquid-to-solid transition may occur when the temperature reaches the liquid–solid coexistence line in the phase diagram. However, the rate of nucleation depends on the surface energy, and the event is driven by the diffusion of the depleted phase into the newly formed phase. Different substances crystallize in various crystal structures that depend on chemical properties and thermodynamic and kinetic conditions such as pressure, temperature, and the structure of the actual surface. One special mode of crystallization is spherulite formation.<sup>2–6</sup> Spherulites are radially oriented polycrystalline complexes that contain branching fibers in a spherical ensemble,<sup>7</sup> and these fibers sometimes can be long whiskers.<sup>8</sup> Their formation is related to crystallization from the melt or solution, and it is controlled by the temperature-gradient-dependent diffusion rate, the chemical structure, and, among other factors, the structure of the substrate on which crystallization occurs.

A few of the first observations on periodic crystallization<sup>9–13</sup> were reported by Fischer-Treuenfeld,<sup>14</sup> who reported the phenomenon of the periodic crystallization of sulfur, and by Hedges with benzophenone, acetanilide, and menthol.<sup>15</sup>

Garner and Randall concluded that the rhythmic solidification occurs due to the temperature differences of crystallization at liquid–air and liquid–glass interfaces.<sup>16</sup> MacMasters and coworkers suggested a simple model for the rhythmic crystallization of different dichromate substances that showed similar Liesegang ring phenomena.<sup>17</sup> Shtukenberg et al. investigated the helical fibril formation of D-mannitol as a function of additive content and temperature and concluded that periodic oscillation of circular birefringence occurs due to the periodic variation of the misorientation of the overlapping lamellae.<sup>18</sup> Benbow and Wood suggested that not only is a high degree of supercooling required for rhythmic solidification to occur but also a large variation in surface tension with temperature is essential.<sup>19</sup> They suggest that the emitted latent heat is passed rapidly onto the surrounding supercooled melt if solidification is started from a highly supercooled liquid. This results in a sudden increase in the local temperature of the melt, which reduces the surface tension and makes the melt flow away from the solid, but after the heat has dissipated, the melt will flow close to the solid, and this repeated process creates a cycle that is manifested in macroscopic patterns. A similar explanation of the latent heat effect was given in a later

**Received:** April 8, 2019

**Revised:** May 28, 2019

**Published:** June 4, 2019

study of Iwamoto et al., who studied the periodic crystallization of ascorbic acid.<sup>20</sup>

Menthol is an optically active organic material that crystallizes in many different forms and has several different enantiomers, among which the most stable enantiomers are (1*R*,2*S*,5*R*)-menthol ((-)-menthol) and (1*S*,2*R*,5*S*)-menthol ((+)-menthol). Some preliminary results were presented by Wright in his early work showing that radial spherulites with spherical shape are formed in the crystallization of menthol.<sup>21</sup> Additionally, Yuasa and coworkers have reported the whisker growth of (-)-menthol.<sup>8</sup> Whisker formation is important in pharmaceuticals because ingredients can grow as whiskers in solid preparations. Some examples have been reported on polyoxymethylene,<sup>22</sup> triglyceride (palm and coconut oil),<sup>23</sup> and carbamazepine.<sup>24</sup>

Bombicz et al. studied (-)-menthol and found that it crystallizes in the trigonal crystal system with space group  $P3_1$ .<sup>25</sup> There are three independent molecules in the asymmetric unit that are constructing three columns. These molecules are organized by hydrogen bondings related by the  $3_1$  screw axis. Single-crystal X-ray diffraction was used to investigate the structure of the (-)-menthol.<sup>25</sup>

The helices and helicoids formed during crystallization are chiral. Whether there is any correlation between the macroscopic chiral morphologies and the molecular configuration is an interesting question,<sup>26</sup> but it is recognized that no direct relationship should be expected. Bernauer found that for twisting there is no need for the components to have optical activity.<sup>27</sup> In some cases, this link can be observed; for example, poly(*R*-3-hydroxybutyrate) always twists to the left.<sup>28</sup> However, this connection is not simple. The twist senses can change with a change in the crystallographic twisting axis<sup>29</sup> or because of small differences in the molecular structure.<sup>30</sup>

In polymers, the spherulites can also be of the radial or ringed type. In the former ones, the fibrils are straight, whereas in ringed spherulites the fibrils are twisted around their longitudinal axes. However, the twisting of the lamellae may not be the only reason for the formation of ringed spherulites. Kyu et al. suggested that as a consequence of the nonlinear diffusion during the crystallization the crystal growth becomes rhythmic, which causes banded spherulites.<sup>31</sup> Takayanagi and Yamashita observed ringed spherulites in the case of poly(ethylene adipate).<sup>32</sup> Padden and Keith found a similar structure in polypropylene (PP). They observed four types of spherulite in PP, of which type IV formed in the temperature interval from 128 to 132 °C and has a ringed structure.<sup>33</sup> Selenium can also form ring spherulites.<sup>34</sup> Some polymers have configurational chirality that can play a role in the twisting of the lamellae. This link between the lamellar twist and the conformational chirality of the polymer has been studied for different polymers, like *R*- and *S*-poly(epichlorohydrin)<sup>35</sup> and poly(lactic acid),<sup>36</sup> and also in some low-molecular-mass polymer nucleating agents such as 1,3:2,4-di-*O*-benzylidene-*D*-sorbitol.<sup>37–39</sup> Wang et al. found that the twisted lamellae of chiral polylactides display opposite handedness. However, the racemic stereocomplex did not form banded spherulites because of the symmetric packing of *L*- and *D*-chain conformations.<sup>36</sup> Xu et al. studied birefringent banded polymer spherulites. They stated that the driving force of lamellar twisting is associated with the unbalanced surface stresses.<sup>40</sup>

From these studies, it can be concluded that there are two main routes for the formation of the ring-banded structures: The first is the helicoidal twisting of radial lamellae that

produces concentric ringed spherulites (e.g., in polymeric systems).<sup>18</sup> The second is the rhythmic crystallization driven by the crystallization coupled to the solvent evaporation<sup>20</sup> or a reaction front propagation.<sup>10</sup> Additionally, the formation of ring-structured patterns can have various physical and chemical origins, even though the physical look of the patterns shares a common characteristic, namely, a ring-banded structure. For instance, the Liesegang rings form due to a cross diffusion of the initially separated ions (having spatial concentration gradient) coupled to their precipitation reaction in gels.<sup>10</sup> The ring formation in ascorbic acid/methanol system is driven by the interplay among evaporation, interfacial tension, and crystallization.<sup>20</sup>

In this study, we investigate experimentally and numerically the banded spherulite formation in the solidification process from the liquid thin film of the two enantiomeric and the racemic forms of menthol. None of the previous work has provided an accurate and comprehensive description or model for the observed phenomena. In this work, we will present a numerical model that can reproduce the macroscopic pattern and the curvature effect even if it does not involve factors such as latent heat or the diffusion of temperature; however, it does consider the fact that phase separation is initiated from a supercooled melt.

## ■ EXPERIMENTAL SECTION

In the typical experiments, ~0.5 g menthol ((-)-menthol, (+)-menthol, or racemic menthol) purchased from Sigma-Aldrich was placed in silica glass vials (diameter: 2.6 cm, length: 7.0 cm), and the sample was heated using a hot plate (Fisher) or a block heater (VWR) until it was completely melted; then, the liquid menthol was spread onto the inside surface of the vials by rotating the vials horizontally. Then, the vials were closed to avoid evaporation of the sample and put back into a vertical position. The samples were cooled at different cooling rates. Slow cooling was achieved by letting the sample cool at the room temperature (22 °C), whereas rapid cooling rates were achieved by putting the vials into a refrigerator (5 °C), a freezer (-12 °C), or liquid nitrogen (-196 °C). Most experiments were carried out in a closed system. The pattern formation was monitored by an image-processing system using a camera (Canon 70D) with a macro objective (Canon EF-S 60 mm f/2.8 macro USM lens), and the final pattern structures were studied by optical microscopy (OM) (VWR) and polarized optical microscopy (POM) (Leica).

## ■ NUMERICAL MODEL

To understand qualitatively the results obtained in experiments, we used the Cahn–Hilliard (CH) equation,<sup>41</sup> which is a powerful tool to describe the phase separation and the periodic and nonperiodic pattern formation in simple or even in more complex chemical systems with mass-transport processes (e.g., diffusion, advection).<sup>42–44</sup> Phenomena occurring in 2D sometimes can be decomposed into fully equivalent 1D problems. 2D planar front propagation can be described by a 1D mathematical model; similarly, circular front propagation can be studied in a 1D polar coordinate system. Therefore, to investigate the curvature effect of the solidification front, we performed numerical simulations in two geometrical orientations: 1D and 1D polar coordinate systems. The CH equation in 1 dimension has the following form

$$\frac{\partial c}{\partial t} = -\lambda \frac{\partial^2}{\partial x^2} \left( ac - c^3 + \frac{\partial c^2}{\partial x^2} \right)$$

where  $c$  and  $x$  are the concentration of a chemical compound and the spatial variable, respectively.  $a$  and  $\lambda$  are thermodynamics and kinetics constants for the phase separation. The CH equation in the 1D polar coordinate has the form

$$\frac{\partial c}{\partial t} = -\lambda \frac{1}{r} \frac{\partial}{\partial r} \left( r \frac{\partial}{\partial r} \left( ac - c^3 + \frac{1}{r} \frac{\partial}{\partial r} \left( r \frac{\partial c}{\partial r} \right) \right) \right)$$

where  $r$  is the radius. The CH equation was solved numerically in both cases in a 1D domain with the method of lines technique (grid spacing,  $\Delta x = \Delta r$  was 1) with the following parameters of the CH equation:  $a = 1.0$  and  $\lambda = 1.0$ . The time integration was performed by using a backward Euler method with the dimensionless time step of 0.01. The initial condition for  $c$  was 0.3 at all grid points, and a small perturbation was applied in  $x = r = 0$  at  $t = 0$  (increasing the value of  $c$  to 1.0). The initial concentration of menthol in the simulations was above the spinodal point, which is a threshold concentration; that is, the system was in a metastable state. When the local concentration of a material reached it, the system started to segregate into high- and low-density phases. In our case, the high- and low-density phases correspond to regions with high- and low-density crystal regions. However, at the beginning of the simulations, the system is metastable, and no phase separation can be observed because of the homogeneous spatial distribution of the concentration, even if the concentration everywhere reaches the spinodal point. In this case, to initiate the phase transition and a solidification front, a perturbation must be applied.

## RESULTS AND DISCUSSION

First, we investigated the pattern formation of (–)-menthol, which started 2 to 10 min after commencing the experiments (by creating a thin liquid film on the inner surface of the vials). In a typical experiment, the formation of concentric rings (ring-banded spherulitic morphology) of menthol could be observed with time (Movie S1), and the obtained pattern was stationary in the wake of the solidification front (Figure 1). In

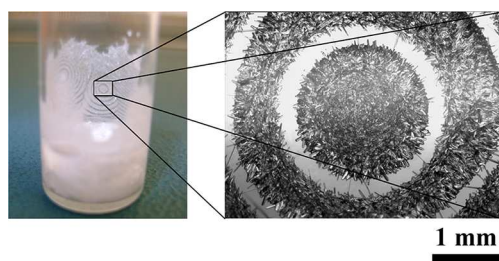


**Figure 1.** (a) Ring-banded spherulitic pattern formation of (–)-menthol in a glass vial (diameter: 2.6 cm, length: 7.0 cm). (b) Optical micrograph of the ring-banded pattern using transmitted light. Darker and lighter regions correspond to the high- and low-density crystal packing, respectively.

most cases, the formation of the pattern started from a point, and the solidification front and the ring formation evolved further from the center. The velocity of the solidification front in the experiments was on the order of  $\sim 0.15$  mm/s. OM revealed that the structure consisted of two periodic regions: a region with tightly packed needle-like crystals of menthol and a practically empty region, where only a few menthol crystals could be found. Sometimes, when the pattern formation started from several centers, the evolving fronts merged

together, forming empty linear edges (Voronoi patterns), which were observed in some other chemical systems (Figure 2).<sup>45,46</sup>

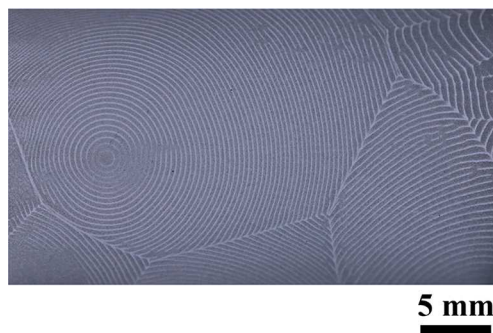


**Figure 2.** Formation of empty linear edges when two solidification fronts of (–)-menthol meet each other in a glass vial (diameter: 2.6 cm, length: 7.0 cm). The photograph was taken using transmitted light illumination. Darker and lighter regions correspond to the high- and low-density crystal packing, respectively.

We tested the effects of the wall size and the volume of the container, and no difference was found in the pattern formation in large (diameter: 2.6 cm, length: 7.0 cm) or small (diameter: 2.0 cm, length: 3.0 cm) vials.

Additionally, we tested several different experimental conditions for the banded spherulite formation. We observed a higher probability for the formation of periodic pattern when the menthol was melted just slightly above its melting point ( $43$  °C)<sup>47</sup> up to about  $50$ – $55$  °C, when the system was closed (sealed by a cap), and when a slow cooling rate was applied (cooling at room temperature). When the cooling rate was too high, that is, the liquid sample was put into the freezer or into liquid nitrogen, the very short cooling time scale did not allow the formation of the solidification front, orientated crystals, or pattern formation.

The periodic growth mechanism can be described as follows. Initially, crystalline fibers start growing from a single point, which facilitates the further growth of menthol crystals due to heterogeneous nucleation and growth. The crystals grow radially at various angles, and menthol molecules from the liquid phase diffuse toward crystals; growing crystals deplete their surroundings, and further crystal growth is hindered. A new nucleation process followed by the crystal growth starts farther from these crystals because of the depleted region; consequently, a new ring of crystals forms.

Experiments were carried out with (+)-menthol as well, and similar results were obtained as those with (–)-menthol (Figure 3a,b). However, in this case the low-density crystal zones are thinner compared with patterns in (–)-menthol, and the crystals of menthol are radially oriented.

The most interesting and striking observation is that the thickness of the bands in the ring-banded spherulite structure decreases with the distance from the center of the rings, and the dependence of the number of rings on their positions measured from the center has nonlinear behavior (Figure 4). This is attributed to the curvature effect of the propagating solidification front. A change in the curvature of the front affects the strength of the diffusion flux, thus affecting the final pattern structure. There are several examples in reaction–diffusion systems in which the curvature affects the dynamics of the pattern formation, especially in cases in which the mass

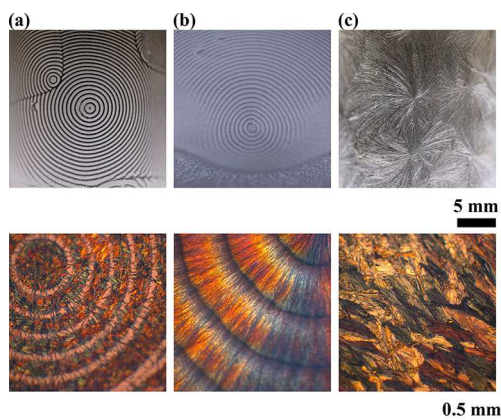


**Figure 3.** Formation of banded spherulites in (a) (–)-menthol, (b) (+)-menthol, and (c) nonbanded spherulites in the racemic mixture of menthol on the inner surface of glass vials with a diameter of 2.6 mm using reflected light illumination. The first and second rows show optical and polarized optical micrographs, respectively.

transport is coupled to the transformation of the chemical compounds. Numerical simulations provide similar results (Figure 4), and these results support the experimental observations of the curvature effect. Additionally, when the front propagates in a planar orientation (no curvature effect)

the thickness of the bands is constant with a value of  $\sim 0.27$  mm, and the dependence of the number of bands on their positions has a strict linear dependence (Figure 5). We obtained similar trends in the numerical simulations (Figure 5). Interestingly, when the curvature decreases (in both experiments and simulations), the width of the rings approaches the constant value of the bands formed in a planar orientation (Figures 4a,b and 5a,b).

Surprisingly, using racemic menthol we have never observed ring-banded spherulitic growth from the liquid film out of 100 experiments (Figure 3c). There is a significant difference between the crystal structures obtained from the crystallization of pure enantiomeric forms and the racemic mixture of menthol. Enantiomers of menthol form long needle-like crystals with an average diameter of a few micrometers, and they self-assemble into a periodic structure by spatially varying the density of needle crystals (Figure 6a). However, racemic menthol preferably forms lamellar crystals that grow spatially, continuously forming spherulites (Figure 6b).

From the experiments carried out in this study, we know that the enantiomeric forms of menthol form ring-banded spherulites; however, their racemic mixture provides non-banded spherulites. We also intended to investigate the effect of the mixing ratio of the two enantiomeric forms of menthol on the formation of the ring-banded spherulites in the solidification process. We prepared several samples with

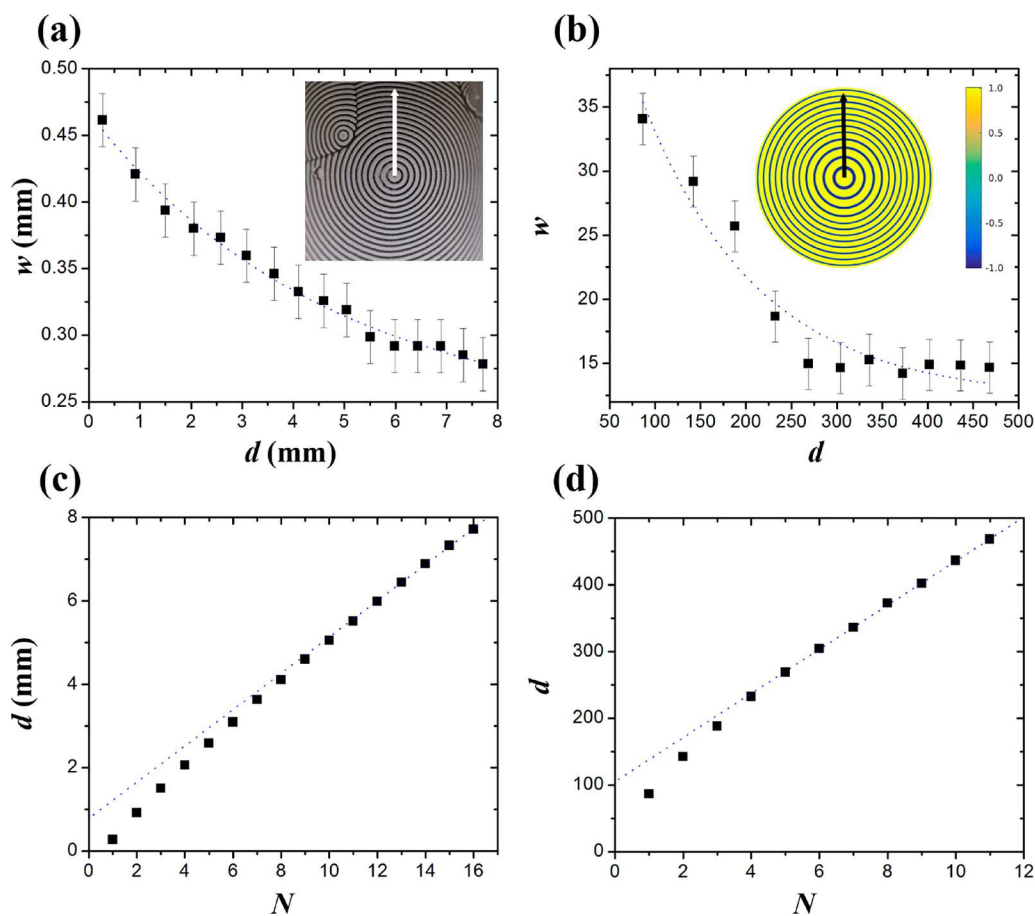


**Figure 4.** Dependence of the width of the bands on the band positions measured from the center in (a) an experiment and (b) a numerical simulation in the case of a radial solidification front propagation. Variation of the position of the bands on band number in (c) experiments and (d) numerical simulations. The error bars correspond to the error of the determination of the width of the bands in experiments and numerical simulations due to the resolution of the experimental images and grid spacing in simulations.

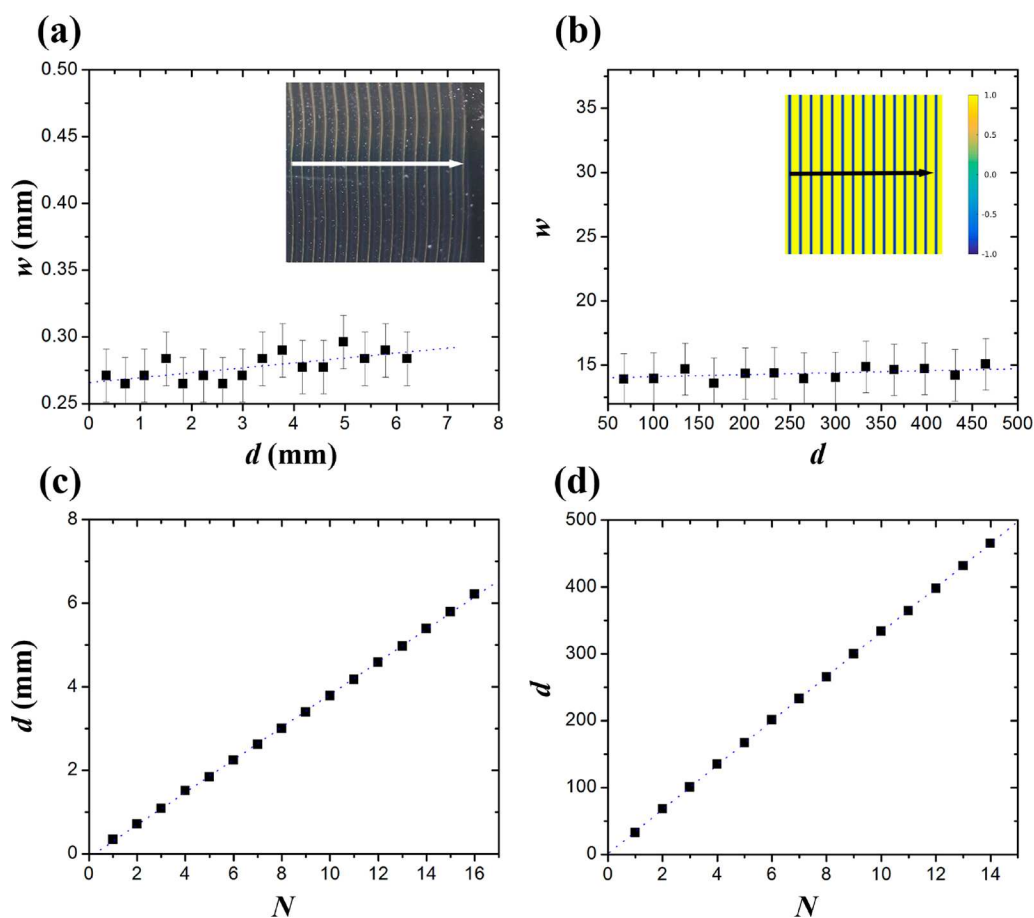


**Figure 5.** Dependence of the width of the bands on the band positions in (a) an experiment and (b) a numerical simulation in the case of a planar solidification front propagation. Variation of the position of the bands on the band number in (c) experiments and (d) numerical simulations. Error bars correspond to the error of the determination of the width of the bands in experiments and numerical simulations due to the resolution of the experimental images and grid spacing in simulations.

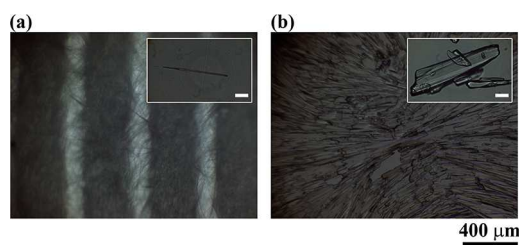


**Figure 6.** Structures of the crystallization patterns formed from (a) (–)-menthol and (b) the racemic mixture of menthol by using optical microscopy (transmitted light illumination). The inset images show the building blocks, and the scale bars in the inset images indicate 20  $\mu\text{m}$ .

various mixing ratios ((+)-menthol: (–)-menthol) of two enantiomeric forms of menthol ranging between 0.01 (1%) and 0.25 (25%); the mixing ratios were the following: 0.01, 0.10, 0.15, 0.20, and 0.25. We observed a ring-banded spherulitic growth to mixing ratio of 0.15; however, we found only nonbanded spherulites from the mixing ratio of 0.20 and higher.

## CONCLUSIONS

We investigated the ring-banded spherulite formation in a thin film of menthol during the liquid-to-solid transition. We found that the enantiomeric pure menthol produces ring-banded

spherulites, whereas their racemic mixture forms only non-banded spherulites. We could clearly identify the curvature effect of the solidification front on a millimeter scale on the pattern formation. Our numerical model qualitatively provided similar results to those observed in the experiments. It is worth noting that in some chemical systems, chirality can develop from the molecular scale to the macroscopic crystal structure (e.g., liquid polymers). In the work of Wang et al., the authors found that the helical molecular configuration is caused by the atomic chiral centers that may result in helical crystals; however, the transfer strongly depends on the packing scheme.<sup>30</sup> The chiral transfer starts at the atomic level, which may cause the secondary chiral structure of the helical configuration that finally results in the macroscopic chirality that could form a banded spherulite structure. However, in our case, the crystals formed from the enantiomeric pure menthols ((–)-menthol and (+)-menthol) have no chirality (long needle-like crystals), and they self-assemble into ring-banded spherulites. Our system shows a simple example of pattern formation that can occur in a one-component system with a simple phase transition, in which the final and stationary pattern depends on the mixing ratio of the enantiomeric forms of menthol.

## ■ ASSOCIATED CONTENT

### Supporting Information

The Supporting Information is available free of charge on the ACS Publications website at DOI: [10.1021/acs.cgd.9b00465](https://doi.org/10.1021/acs.cgd.9b00465).

Movie S1. Formation of the ringed-banded structure in the solidification front of (–)-menthol (MOV)

## ■ AUTHOR INFORMATION

### Corresponding Author

\*E-mail: [istvanlagzi@gmail.com](mailto:istvanlagzi@gmail.com). Tel: +361-463-1341. Fax: +361-463-4180.

### ORCID

Hugo K. Christenson: [0000-0002-7648-959X](https://orcid.org/0000-0002-7648-959X)

Istvan Lagzi: [0000-0002-2303-5965](https://orcid.org/0000-0002-2303-5965)

### Notes

The authors declare no competing financial interest.

## ■ ACKNOWLEDGMENTS

This study was supported by the National Research, Development and Innovation Office of Hungary (NN125752) and the BME-Nanotechnology FIKP grant of EMMI (BME FIKP-NAT). H.K.C. acknowledges support from the Leverhulme Trust (grant F/10101/B). We thank Professor Zoltán Rác (Eötvös University) for the helpful discussion.

## ■ REFERENCES

- Benbow, J. J.; Wood, D. J. C. Unusual Liquid-Solid Transition Effects in a Methoxypentamethylflavan. *Proc. R. Soc. London Ser. Math. Phys. Sci.* **1958**, *243*, 518–533.
- Goldenfeld, N. Theory of Spherulitic Crystallization. *J. Cryst. Growth* **1987**, *84*, 601–608.
- Buckley, H. E. *Crystal Growth*; John Wiley: New York, 1951.
- Gránásy, L.; Pusztai, T.; Tegze, G.; Warren, J. A.; Douglas, J. F. Growth and Form of Spherulites. *Phys. Rev. E* **2005**, *72*, 11605.
- Gránásy, L.; Pusztai, T.; Börzsönyi, T.; Warren, J. A.; Douglas, J. F. A General Mechanism of Polycrystalline Growth. *Nat. Mater.* **2004**, *3*, 645.
- Crist, B.; Schultz, J. M. Polymer Spherulites: A Critical Review. *Prog. Polym. Sci.* **2016**, *56*, 1–63.
- Magill, J. H. Review Spherulites: A Personal Perspective. *J. Mater. Sci.* **2001**, *36*, 3143–3164.
- Yuasa, H.; Ooi, M.; Takashima, Y.; Kanaya, Y. Whisker Growth of L-Menthol in Coexistence with Various Excipients. *Int. J. Pharm.* **2000**, *203*, 203–210.
- Brumbergeb, H. Rhythmic Crystallization of Poly-L-Alanine. *Nature* **1970**, *227*, 490–491.
- Packter, A. The Effect of Crystallinity on Rhythmic Precipitation. *J. Chem. Soc.* **1955**, 1180–1184.
- Dippy, J. F. J. The Rhythmic Crystallization of Melts. *J. Phys. Chem.* **1931**, *36*, 2354–2361.
- Menzies, A. W. C.; Sloat, C. A. Spiral Markings on Carborundum Crystals. *Nature* **1929**, *123*, 348–349.
- Iwamoto, K.; Mitomo, S.; Fukide, J.; Shigemoto, T.; Seno, M. Pattern Formation by Rhythmic Crystallization of Methyl Mesityl-carbamate. *Bull. Chem. Soc. Jpn.* **1982**, *55*, 709–712.
- Fischer-Treuenfeld, A. v. Rhythmenbildung Bei Der Erstarrung Des Schwefels. *Colloid Polym. Sci.* **1915**, *16*, 109–111.
- Hedges, E. S. Periodic and Spiral Forms of Crystallisation. *Nature* **1929**, *123*, 837.
- Garner, W. E.; Randall, F. C. XLIV.—The Rhythmic Crystallisation of Undecic Acid. *J. Chem. Soc., Trans.* **1924**, *125*, 369–372.
- MacMasters, M. M.; Abbott, J. E.; Peters, C. A. Investigations of the Effects of Some Factors on Rhythmic Crystallization I. *J. Am. Chem. Soc.* **1935**, *57*, 2504–2508.

(18) Shtukenberg, A. G.; Cui, X.; Freudenthal, J.; Gunn, E.; Camp, E.; Kahr, B. Twisted Mannitol Crystals Establish Homologous Growth Mechanisms for High-Polymer and Small-Molecule Ring-Banded Spherulites. *J. Am. Chem. Soc.* **2012**, *134*, 6354–6364.

(19) Benbow, J. J.; Wood, D. J. C. Unusual Liquid-Solid Transition Effects in a Methoxypentamethylflavan. *Proc. R. Soc. London Ser. Math. Phys. Sci.* **1958**, *243*, 518–533.

(20) Iwamoto, K.; Mitomo, S.-I.; Seno, M. Rhythmic Crystallization of Ascorbic Acid Precipitated from Its Methanol Solutions. *J. Colloid Interface Sci.* **1984**, *102*, 477–482.

(21) Wright, F. E. The Crystallization of Menthol. *J. Am. Chem. Soc.* **1917**, *39*, 1515–1524.

(22) Van Der Heijde, H. B. Whisker-like Growth of Polyoxymethylene from Solution. *Nature* **1963**, *199*, 798–799.

(23) Okada, M. Whisker-like Growth of Triglyceride. *J. Cryst. Growth* **1970**, *7*, 371–374.

(24) Laine, E.; Tuominen, V.; Ilvessalo, P.; Kahela, P. Formation of Dihydrate from Carbamazepine Anhydrate in Aqueous Conditions. *Int. J. Pharm.* **1984**, *20*, 307–314.

(25) Bombicz, P.; Buschmann, I. J.; Luger, P.; Dung, N. X.; Nam, C. B. Crystal Structure of (1R,2S,5R)-2-Isopropyl-5-Methyl-Cyclohexanol, (–)-Menthol. *Z. Kristallogr. - Cryst. Mater.* **1999**, *214*, 420.

(26) Shtukenberg, A. G.; Punin, Y. O.; Gujral, A.; Kahr, B. Growth Actuated Bending and Twisting of Single Crystals. *Angew. Chem., Int. Ed.* **2014**, *53*, 672–699.

(27) Bernauer, F. "Gedrillte" Kristalle; Verbreitung, Entstehungsweise und Beziehungen zu optischer Aktivität und Molekülsymmetrie; Gebrüder Borntraeger: Berlin, 1929.

(28) Saracovan, I.; Keith, H. D.; Manley, R. S. J.; Brown, G. R. Banding in Spherulites of Polymers Having Uncompensated Main-Chain Chirality. *Macromolecules* **1999**, *32*, 8918–8922.

(29) Ye, H.-M.; Xu, J.; Guo, B.-H.; Iwata, T. Left- or Right-Handed Lamellar Twists in Poly[(R)-3-Hydroxyvalerate] Banded Spherulite: Dependence on Growth Axis. *Macromolecules* **2009**, *42*, 694–701.

(30) Wang, J.; Li, C. Y.; Jin, S.; Weng, X.; Van Horn, R. M.; Graham, M. J.; Zhang, W. B.; Jeong, K. U.; Harris, F. W.; Lotz, B.; Cheng, S. Z. D. Helical Crystal Assemblies in Nonracemic Chiral Liquid Crystalline Polymers: Where Chemistry and Physics Meet. *Ind. Eng. Chem. Res.* **2010**, *49*, 11936–11947.

(31) Kyu, T.; Chiu, H. W.; Guenther, A. J.; Okabe, Y.; Saito, H.; Inoue, T. Rhythmic Growth of Target and Spiral Spherulites of Crystalline Polymer Blends. *Phys. Rev. Lett.* **1999**, *83*, 2749–2752.

(32) Takayanagi, M.; Yamashita, T. Growth Rate and Structure of Spherulite in Fractionated Poly(ethylene Adipate). *J. Polym. Sci.* **1956**, *22*, 552–555.

(33) Padden, F. J.; Keith, H. D. Spherulitic Crystallization in Polypropylene. *J. Appl. Phys.* **1959**, *30*, 1479–1484.

(34) Fitton, B.; Griffiths, C. H. Morphology of Spherulites and Single Crystals of Trigonal Selenium. *J. Appl. Phys.* **1968**, *39*, 3663–3671.

(35) Singfield, K. L.; Brown, G. R. Optically Active Polyethers. I. Studies of the Crystallization in Blends of the Enantiomers and the Stereoblock Form of Poly(epichlorohydrin). *Macromolecules* **1995**, *28*, 1290–1297.

(36) Wang, H.-F.; Chiang, C.-H.; Hsu, W.-C.; Wen, T.; Chuang, W.-T.; Lotz, B.; Li, M.-C.; Ho, R.-M. Handedness of Twisted Lamella in Banded Spherulite of Chiral Polylactides and Their Blends. *Macromolecules* **2017**, *50*, 5466–5475.

(37) Terech, P.; Weiss, R. G. Low Molecular Mass Gelators of Organic Liquids and the Properties of Their Gels. *Chem. Rev.* **1997**, *97*, 3133–3160.

(38) Thierry, A.; Straupé, C.; Wittmann, J.-C.; Lotz, B. Organogelators and Polymer Crystallisation. *Macromol. Symp.* **2006**, *241*, 103–110.

(39) Thierry, A.; Fillon, B.; Straupé, C.; Lotz, B.; Wittmann, J. C. Polymer Nucleating Agents: Efficiency Scale and Impact of Physical Gelation. In *Solidification Processes in Polymers*; Jansson, J.-F., Gedde, U. W., Eds.; Steinkopff, 1992; pp 28–31.

- (40) Xu, J.; Ye, H.; Zhang, S.; Guo, B. Organization of Twisting Lamellar Crystals in Birefringent Banded Polymer Spherulites: A Mini-Review. *Crystals* **2017**, *7*, 241.
- (41) Cahn, J. W.; Hilliard, J. E. Free Energy of a Nonuniform System. I. Interfacial Free Energy. *J. Chem. Phys.* **1958**, *28*, 258–267.
- (42) Antal, T.; Droz, M.; Magnin, J.; Rácz, Z. Formation of Liesegang Patterns: A Spinodal Decomposition Scenario. *Phys. Rev. Lett.* **1999**, *83*, 2880–2883.
- (43) Rácz, Z. Formation of Liesegang Patterns. *Phys. A* **1999**, *274*, 50–59.
- (44) Thomas, S.; Lagzi, I.; Molnár, F.; Rácz, Z. Probability of the Emergence of Helical Precipitation Patterns in the Wake of Reaction-Diffusion Fronts. *Phys. Rev. Lett.* **2013**, *110*, 78303.
- (45) Tolmachiev, D.; Adamatzky, A. Chemical Processor for Computation of Voronoi Diagram. *Adv. Mater. Opt. Electron.* **1996**, *6*, 191–196.
- (46) Zámbo, D.; Suzuno, K.; Pothorszky, S.; Bárdfalvy, D.; Holló, G.; Nakanishi, H.; Wang, D.; Ueyama, D.; Deák, A.; Lagzi, I. Self-Assembly of like-Charged Nanoparticles into Voronoi Diagrams. *Phys. Chem. Chem. Phys.* **2016**, *18*, 25735–25740.
- (47) Corvis, Y.; Négrier, P.; Massip, S.; Leger, J.-M.; Espeau, P. Insights into the Crystal Structure, Polymorphism and Thermal Behavior of Menthol Optical Isomers and Racemates. *CrystEngComm* **2012**, *14*, 7055–7064.